Experimental Assessment of PowerFeed Chromatography

Ziyang Zhang and Massimo Morbidelli
Swiss Federal Institute of Technology Zurich, Institute for Chemical and Bio-Engineering, ETH-Hönggerberg/HCI, CH-8093 Zurich, Switzerland

Marco Mazzotti
ETH Zurich, Institute of Process Engineering, Sonneggstrasse 3, CH-8092, Zurich, Switzerland

The PowerFeed process is a modification of the simulated moving bed (SMB) technique, where the flow rates in the unit are allowed to change during a switching period following a predefined pattern. Through multiobjective optimization, using a genetic algorithm, it is shown that PowerFeed achieves better performances than SMB in several cases of interest for applications. Moreover, its experimental feasibility and effectiveness is assessed by running and comparing SMB and PowerFeed separations of the enantiomers of α-ionone, on a cyclodextrin based chiral stationary phase. © 2004 American Institute of Chemical Engineers *AIChE J,* 50: 625–632, 2004
Keywords: PowerFeed process, simulated moving bed, experiment, multiobjective optimization, process design, chiral separation

Introduction

Simulated moving bed (SMB) is a continuous adsorption based separation technique covering numerous applications, which are difficult or even impossible to address using other separation techniques. In particular, SMB meets the increasing needs for the rapid and reliable development of new pure enantiomeric pharmaceuticals (Juza et al., 2000).

Originally, the SMB process was devised as the practical implementation of a true moving bed (TMB) unit, where the solid adsorbent phase and the fluid phase move countercurrently (Ruthven and Ching, 1989; Storti et al., 1993; Mazzotti et al., 1997a). Recently, SMBs with new operation modes have been investigated, aiming at reducing its production cost and improving its separation efficiency. These include supercritical fluid SMB (Nicoud et al., 1993; Mazzotti et al., 1997b; Di Giovanni et al., 2001; Denet et al., 2001), temperature gradient SMB (Migliorini et al., 2001), and solvent gradient SMB (Jensen et al., 2000; Antos and Seidel-Morgenstern, 2001; Abel et al., 2002). The basic idea is to change the adsorption strength of the solutes on the stationary phase in the different sections, by creating along the unit a gradient of operating conditions, that is, temperature, pressure or solvent power.

Another direction to improve SMB performance is based on the idea of modifying the dynamic characteristics of its operation, using time varying solid and liquid flow rates instead of the constant ones of the standard SMB process. In this way, a SMB unit is no longer equivalent to a TMB unit with five degrees of freedom, that is, internal fluid flow rates Q_1 to Q_4 and switching time t^*, but can be regarded as a unit by itself with a larger number of degrees of freedom. One proposition in this direction is the Varicol unit (Ludemann-Hombourger et al., 2000, 2002; Zhang et al., 2002, 2003a), where the inlet and outlet ports are shifted asynchronously, thus being somehow equivalent to a TMB where the solid phase flow rate varies in time during each switching period. A second proposition is that of allowing the fluid flow rates to vary during the switching period (Kearney and Hieb, 1992; Kloppenburg and Gilles, 1999; Zang and Wankat, 2002a,b; Zhang et al., 2003b). Since the most important flow rate modulation is that of the feed flow

Correspondence concerning this article should be addressed to M. Morbidelli at morbidelli@tech.chem.ethz.ch.

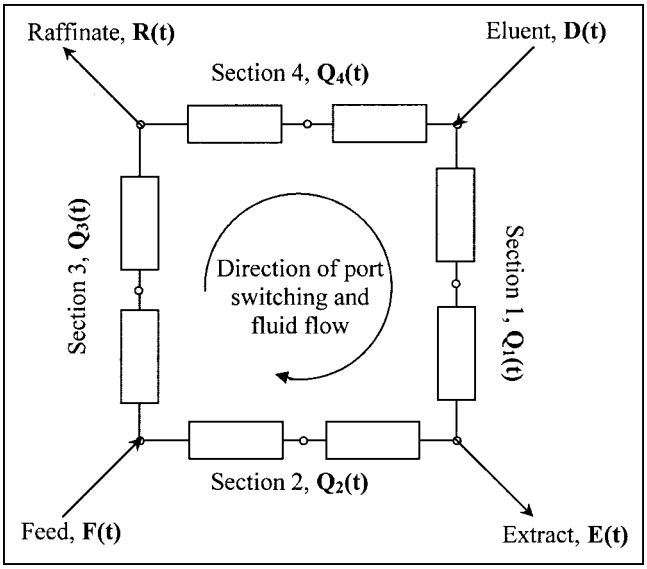

Figure 1. Four section PowerFeed unit.

rate, and this implementation of the SMB technology yields improved productivity, we call it the PowerFeed process (Zhang et al., 2003b). Figure 1 shows the scheme of a PowerFeed unit, which is the same as that of a SMB unit, except that the fluid flow rates change in time. Since only four of the eight internal and external fluid flow rates are independent, we can force at most four flow rates, such as Q_1, Q_2, F and D, to vary, while the other four flow rates follow from the mass balance, that is $Q_3 = Q_2 + F$, $Q_4 = Q_1 - D$, $R = Q_3 - Q_4$, $E = Q_1 - Q_2$. More recently, a third SMB operation of this type has been proposed, where additional degrees of freedom are obtained by modulating the feed concentration during the switching period (Schramm et al., 2002, 2003).

A detailed analysis based on multiobjective optimization has shown that the PowerFeed performs better than the SMB in terms of raffinate and extract product purities, and, for the same productivity, eluent consumption, and amount of stationary phase, in the case of both linear and nonlinear systems (Zhang et al., 2003b). This is particularly significant when only a small number of columns is used. However, no general rule has been found on how to vary the fluid flow rates, and no experimental result is available to validate the above theoretical findings.

The main objective of this work is to investigate the separation performance of the PowerFeed process experimentally. The separation of the enantiomers of α-ionone, a norterpenoid ketone, which is an important compound in perfumery, flavor, and fragrance technology (Quattrini et al., 1999), is conducted in an open-loop HPCL-SMB laboratory unit. It is worth noting that, in the open-loop case, $Q_1 = D$ by definition. In order to keep the experimental set up relatively simple, a simplified PowerFeed operation is considered, where the feed flow rate F only is varied, whereas Q_1, Q_2, and Q_4 are kept constant (see Figure 2a); as a result, Q_3 and R vary in time. The F variation is further limited to step changes in three subintervals of equal length during each switching period, with F_1, F_2 and F_3 being the feed flow rates in each subinterval. Since Q_2 and Q_4 are fixed, a change in F results in a corresponding change in Q_3 and R as illustrated in Figure 2b.

It is worth underlying how this article adds to previous contributions on SMB operation with time varying flow rates. Such a concept was introduced in a very general form in a patent, where the application was limited to sugar separations (Kearney and Hieb, 1992). Thus, it was considered again from a theoretical viewpoint for the separation of xylenes (Kloppenburg and Gilles, 1999). More recently, a detailed theoretical analysis of the special case where only the feed flow rate is changed in an on-off fashion, was reported for a linear system (Zang and Wankat, 2002a). In our previous contribution (Zhang et al., 2003b), we have considered through numerical optimization, the general case where all flow rates can change in time, including the analysis of both linear and competitive nonlinear systems. In this article, the PowerFeed operation is applied and validated experimentally, particularly for the important case of the separation of the enantiomers of a chiral compound.

Materials and Methods

Racemic α-ionone (purity 90%) was obtained from Fluka (Buchs, Switzerland). The impurity in the feed is the nonchiral isomer of α-ionone, that is, β-ionone (Quattrini et al., 1999). The solvent, methanol, HPLC purity grade, was purchased from J. T. Baker (Deventer, Holland), and double distilled water was prepared in the laboratory.

The HPLC-SMB unit used in this work has been described previously (Pedeferri et al., 1999; Zenoni et al., 2002). It consists of eight HPLC columns (12.5 × 1 cm) packed with the stationary phase Nucleodex®-β-PM of particle diameter 10 μm

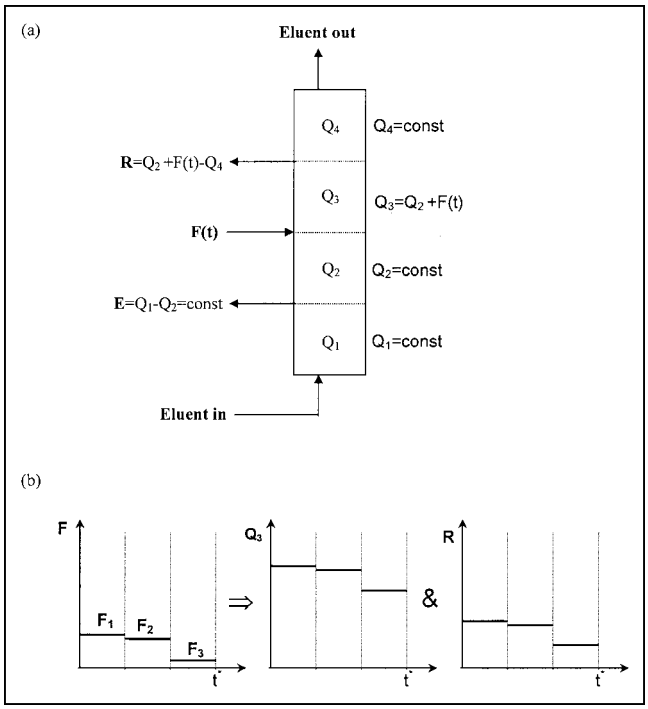

Figure 2. PowerFeed process operating with the feed flow rate, *F* changing in time and constant Q_1, Q_2 and Q_4.

(a) Internal and external fluid flow rates; (b) example of a three-step change in F, and the consequent step changes in Q_3 and R.

Table 1. Experimental and Model Results for the SMB Separation of α-Ionone Enantiomers (c_T^F = 1.14 g/L)

		Flow Rate (mL/min)				t^*	Flow Rate Ratio Parameters				Experiment		Model	
Process	Run	Q_1	Q_2	F_{SMB}	Q_4	(min)	$\bar{m}_1$	$\bar{m}_2$	$\bar{m}_3$	$\bar{m}_4$	P_R, %	P_E, %	P_R, %	P_E, %
SMB	S1	4.082	2.383	0.307	1.845	6.5	5.318	1.773	2.747	1.128	97.25	90.32	96.53	89.68
	S2	4.083	2.383	0.307	1.847	6.7	5.539	1.901	2.891	1.231	88.06	92.08	87.51	91.68
	S3	4.085	2.384	0.307	1.846	6.9	5.762	2.030	3.037	1.328	78.90	92.92	80.90	93.32
	S4	4.071	2.378	0.307	1.841	7.0	5.845	2.083	3.098	1.368	74.44	93.55	78.64	93.87

from Macherey-Nagel (Düren, Germany). The eight columns are located in a thermostatic chamber to guarantee isothermal operation. Two HPLC pumps (Jasco PU-987 and PU-1586, Japan) and a flow mixer (DMC-2000 provided by OmniLab, Switzerland) provide the eluent with the desired composition in methanol and water. Three other HPLC pumps (Jasco PU-987) control the feedstream, as well as two of the three outlet streams, that is, extract and raffinate. The flow rate of the eluent out of section 4, that is, flow rate Q_4, is determined by the overall mass balance since the unit is operated in the open-loop configuration. Five (12 + 1)-port multiposition valves (Vici-Valco EMT-6-CSD12UW, USA) are connected to each of the eight columns to implement the periodic port switch. The SMB and PowerFeed operations are automated using the software package Labview® (National Instruments, TX), which enables all pumps to vary their set points in the prescribed number of evenly distributed subintervals during each switching period.

SMB and PowerFeed experiments were conducted at a temperature of 20°C in an open-loop system with column configuration 1-1-2-4. Note that since, in this system, the desorbent is not recycled and always fed fresh, this unit behaves like a closed-loop system with the same number of columns in the first three sections, and operated in such a way that the desorbent is fully regenerated in section 4, that is, pure desorbent is recycled back to the unit. The bed void fraction is $\varepsilon^* = 0.62$ (Zenoni et al., 2002). The extra-column dead volumes V_j^D were measured to be 0.605, 2.788, 1.150, and 1.696 mL for each column in section 1, 2, 3, and 4, respectively. The difference in these four values is due to the port and valve arrangement between two SMB columns; this, in fact, includes in series, the outlet ports (extract, raffinate, and solvent to be recycled from the outlet of section four), a check valve, and the inlet ports (feed and fresh solvent) (Migliorini et al., 1999). A methanol/water mixture 70/30 (v/v) was used as the mobile phase, and the total feed concentration was 1.14 g/L. Samples from raffinate, extract, and outlet of section 4 were taken during the 18th, 20th and 22nd cycles; the corresponding average purities are reported in the following. Fulfillment of the component material balance has been carefully checked, and an average error of 2% was measured.

Analysis was carried out in a HP 1,100 system (Hewlett-Packard), equipped with a DAD UV detector (wavelength:230 nm) using a Nucleodex®-β-PM HPLC column (Macherey-Nagel, 20 × 0.4 cm; particle diameter, 5 μm). A mixture of methanol and water (65/35 v/v) was used as the mobile phase, with a flow rate of 0.5 mL/min, at a column temperature of 20°C.

Results and Discussion

SMB experiments and model parameters estimation

First, four SMB experiments (runs S1 to S4) were carried out at four switching time values (t^* = 6.5, 6.7, 6.9 and 7.0 min) and constant flow rates Q_1, Q_2, Q_4, and F_{SMB}. The operating conditions and separation performances are reported in Table 1, together with the flow rate ratio parameters $\bar{m}_j$ in the four sections of the unit, calculated including the extra-column dead volume as follows (Migliorini et al., 1999)

$$\bar{m}_j = \frac{Q_j t^* - V\varepsilon^* - V_j^D}{V(1-\varepsilon^*)} \tag{1}$$

It is worth noting that the feed impurity β-ionone has a retention behavior similar to that of the more retained enantiomer of α-ionone, that is, component A in the following. In view of the scope of this work, we have not purified the feed mixture from β-ionone, which is therefore always collected together with component A. Note that the purities values P_E and P_R given in Table 1 and in the following, are computed on a β-ionone free basis.

In order to find the optimal time variation policy for the feed flow rate F in the PowerFeed process, a multiobjective optimization using a genetic algorithm has been used (Bhaskar et al., 2000; Zhang et al., 2002). A stage model was used to simulate the SMB and PowerFeed processes, based on the flow rate ratio parameter $\bar{m}_j$ which accounts for the dead volumes (Zhang et al., 2003a). The adsorption isotherm parameters and the number of theoretical stages, N, have been estimated from the SMB experimental results (runs S1 to S4) by minimizing the difference between the experimental purities and those predicted by the stage model. Using the Langmuir isotherm, that is

$$q_i = \frac{H_i c_i}{1 + K_A c_A + K_B c_B} \tag{2}$$

the isotherm parameters and the number of theoretical stages per column, were estimated to be given by $H_B = 3.24$, $H_A = 5.29$, $K_B = 0.03$, $K_A = 2.02$, and $N = 40$, respectively. The purities calculated by the stage model are consistent with the SMB experimental results, as shown in Table 1 and Figure 3. Some discrepancy is most likely due to the fact that the Langmuir isotherm utilized here provides only an approximation of the actual competitive adsorption behavior of the system under examination.

The operating points of the SMB experiments are shown in the ($\bar{m}_2$, $\bar{m}_3$) plane in Figure 4, and compared to the nonlinear

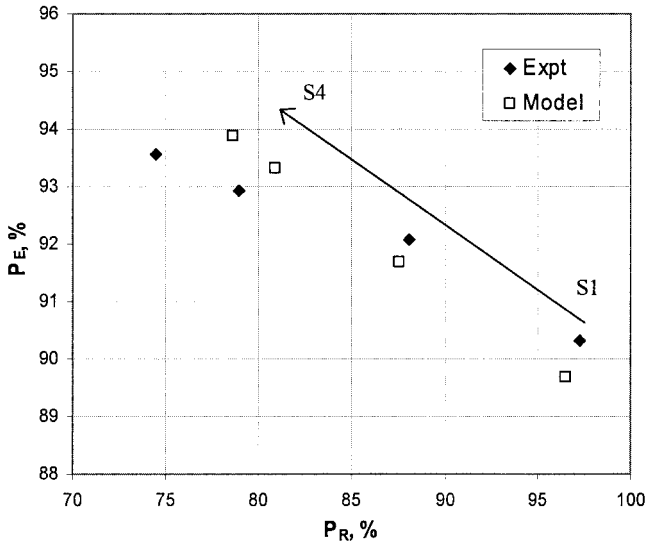

Figure 3. Comparison of experimental and calculated purities in extract and raffinate for a SMB operation.

complete separation region plotted, based on the experimental feed concentration c_T^F, and the adsorption parameters estimated above (Mazzotti et al., 1997a). As the switching time t^* increases from run S1 to S4, according to Eq. 1, both $\bar{m}_2$ and $\bar{m}_3$ increase, and the operating point in the ($\bar{m}_2$, $\bar{m}_3$) plane moves on a straight line going from the pure raffinate to the pure extract region. Accordingly, in the experimental and simulation results reported in Table 1, the extract purity P_E increases and the raffinate purity P_R decreases. It should be noted that no pure streams were obtained in these experiments, because all the operating points were above the complete separation region, as shown in Figure 4.

Comparison of SMB and PowerFeed performance at constant switching time

In this section we compare different PowerFeed runs with the single SMB run S1, using the same Q_1, Q_2, Q_4 and t^* values, but varying the feed flow rate F in three subintervals during the switching period t^*, as shown in Figure 2b. In order to compare the two processes with the equal productivity, the average PowerFeed feed flow rate, $\bar{F}$ is constrained to be the same as the SMB feed flow rate F_{SMB}, so that only two of the three variables, F_1, F_2 and F_3, are independent.

Numerical optimizations have been carried out in order to identify the optimal variation policy for F_i. Such constrained multiobjective optimization can be formally defined as follows

$$\text{Max } J_1 = P_R\,[F_1, F_2] \tag{3a}$$

$$\text{Max } J_2 = P_E\,[F_1, F_2] \tag{3b}$$

subject to Q_1, Q_2, Q_4, F_{SMB}, t^* given as in SMB run S1 in Table 1, and

$$\bar{F} = F_{\text{SMB}};\ F_3 = 3\bar{F} - F_1 - F_2;\ Q_{3,k} = Q_2 + F_k;$$
$$R_k = Q_{3,k} - Q_4\ (k = 1, 2, 3) \tag{3c}$$

In other words, the relationships above require that the raffinate purity, P_R, and the extract purity P_E, be maximized simultaneously by choosing the most convenient F variation policy, but under conditions leading to the same productivity and eluent consumption as in the corresponding SMB run S1. The quantities F_1 and F_2 are the decision variables, while F_3 is fixed by Eq. 3c. Flow rates Q_3 and R in the k$^{\text{th}}$ subinterval (k = 1, 2, 3) are given through Q_2, Q_4, and the corresponding F_k value by the overall balances at the nodes of the unit. The multiobjective optimization problem is solved using a nondominated sorting genetic algorithm (NSGA) (Bhaskar et al., 2000; Zhang et al., 2002).

The optimization results, that is, the maximum P_R and P_E values achievable with the PowerFeed process under the conditions above, are plotted and compared to the simulated results of the SMB run S1 in Figure 5a. It is worth noting that the PowerFeed results in Figure 5a constitute a Pareto curve, which indicates that, for increasing raffinate purity, the optimal extract purity decreases. Moreover, the PowerFeed operation is always better than the SMB operation in one or the other of P_R and P_E, but only in a very few cases in both. Obviously, different points in the PowerFeed Pareto set of Figure 5a correspond to different feed flow rate variation policies. This is illustrated in Figure 5b where the values of F_1, F_2, and F_3 corresponding to the optimal performance shown in Figure 5a are reported as a function of P_R. It is evident that, in the PowerFeed operation, the higher extract purity values, that is, lower P_R, are achieved when the whole amount fed to the SMB unit during the entire switching period, that is, $F_{\text{SMB}}t^*$, is fed during the first subinterval, that is, where $F_1 \cong 3F_{\text{SMB}}$ and $F_2 \cong F_3 \cong 0$. On the contrary, the higher P_R values require that

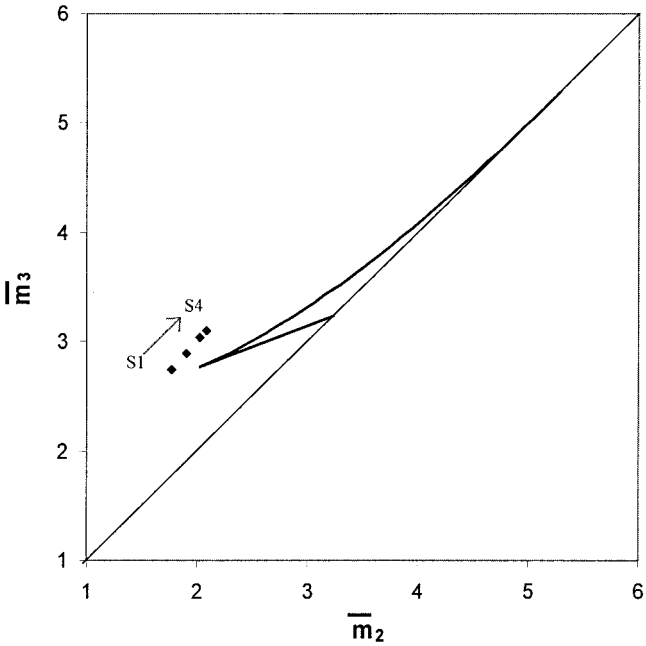

Figure 4. Operating points of the SMB experimental runs (S1 to S4 in Table 1) in the ($\bar{m}_2$, $\bar{m}_3$) plane.

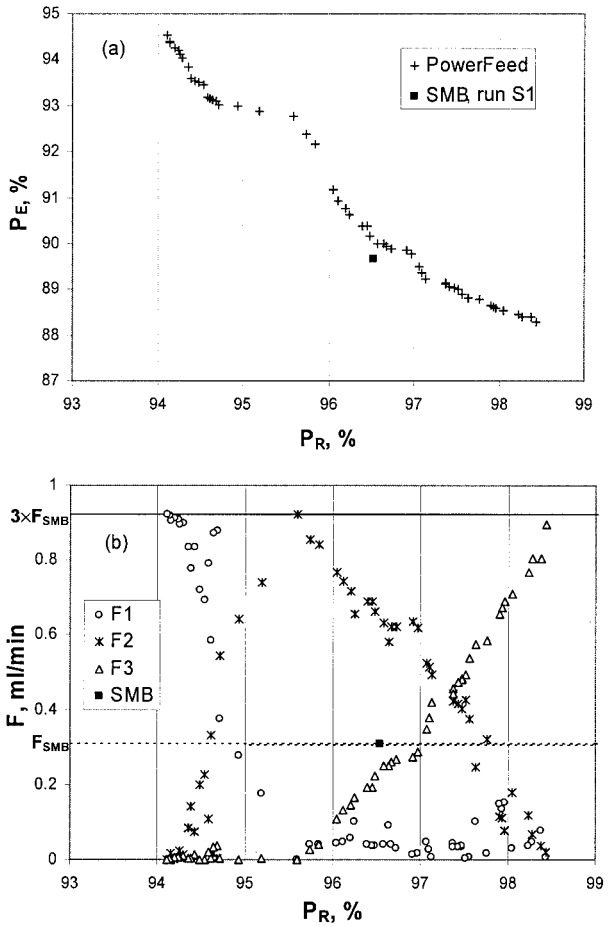

Figure 5. Comparison between the Pareto solution of the PowerFeed optimization problem (Eq. 3), and the simulation of the SMB run S1.

$F_3 \cong 3F_{SMB}$ and $F_1 \cong F_2 \cong 0$. Intermediate P_R values correspond to $F_2 \cong 3F_{SMB}$ and $F_1 \cong F_3 \cong 0$. A similar trend was obtained previously for a linear system (Zang and Wankat, 2002a). Accordingly, it can be observed in Figure 5b that F_1 monotonically decreases while F_3 increases with P_R, whereas F_2 goes through a maximum. It is worth noting that none of the PowerFeed optimal operating conditions on the Pareto set of Figure 5a applies the SMB operation policy, which would correspond to the case where $F_1 = F_2 = F_3 = F_{SMB}$. Accordingly, although very close to the Pareto set, the point in Figure 5a corresponding to run S1 does not belong to it.

In order to verify the observations above, four PowerFeed experiments, with the same Q_1, Q_2, Q_4, and t^* values as the SMB run S1, were carried out using four different F variation policies, which correspond to different time variations of Q_3 (although with the same time average value). The experimental operating conditions and results, as well as the corresponding purity values predicted by the model, are reported in Table 2 (runs P1 to P4). The results in Table 2 confirm that the trends predicted by the model are also observed in the experiments. The agreement between calculated and experimental purity values is similar to that achieved for the SMB experiments discussed in the context of Table 1, and, clearly, it could not be better, since the model parameters are fitted on those SMB experiments. When comparing the performance of runs P1 to P4 with that of run S1, it is readily seen that the PowerFeed runs improve either P_R or P_E, but not both together as in most of the cases illustrated in Figure 5a. Finally, it is worth observing that experiments P3 and P4 are carried out under practically the same operating conditions and represent a confirmation of the reproducibility of the PowerFeed experiments.

Comparison of SMB and PowerFeed performance at varying switching time

The comparison between SMB and PowerFeed performances presented in the previous section was carried out under the constraints of constant switching time t^* and constant flow rates, namely constant Q_1, Q_2, and Q_4, and average Q_3. As to the flow rates, this is indeed a fair comparison since the constant flow rate requirement implies that the compared SMB and PowerFeed runs operate with the same average column efficiency and pressure drop, which in fact, both depend only on the flow rates. Accordingly, changing the switching time t^* at constant flow rates would not affect column efficiency and pressure drop. It is meaningful, both conceptually and from a practical viewpoint, to investigate and compare the two operations in a broader sense, that is, for a range of switching time values. The result of this analysis for the SMB operation has been discussed in the context of Figure 3; and, in the following, we will compare it with the equivalent analysis for the PowerFeed operation. However, due to packing stability, it is to be kept in mind that pressure drop limitations, have to be accounted for with reference to the maximal flow rates in the columns, and not to the average ones. In this work such pressure drop constraint is never limiting.

For the sake of simplicity, only the eight feed flow rate variation policies reported in Table 3 (PF1 to PF8) have been considered. They are representative of the different F_1-F_2-F_3 combinations yielding different P_R and P_E values in Figure 5b. In particular, PF1 and PF2 have large F_1 values, PF4 and PF5 refer to large F_2, while large F_3 values are considered in PF7 and PF8.

Table 2. Experimental and Model Results of the PowerFeed Separation of α-Ionone Enantiomers (c_T^F = 1.14 g/L)

		Flow Rate (mL/min)						t^*	Experiment		Model	
Process	Run	Q_1	Q_2	F_1	F_2	F_3	Q_4	(min)	P_R, %	P_E, %	P_R, %	P_E, %
PowerFeed	P1	4.077	2.377	0.000	0.409	0.512	1.839	6.5	97.38	89.38	98.33	88.77
	P2	4.082	2.381	0.921	0.000	0.000	1.845	6.5	94.15	93.74	94.31	94.46
	P3	4.075	2.376	0.461	0.460	0.000	1.845	6.5	96.91	92.02	95.54	92.88
	P4	4.078	2.380	0.409	0.512	0.000	1.840	6.5	97.05	92.83	95.09	92.99
	P5	4.086	2.385	0.409	0.512	0.000	1.848	6.7	90.76	94.15	86.07	95.50
	P6	4.080	2.380	0.409	0.512	0.000	1.840	6.9	75.95	94.61	80.16	97.08
	P7	4.067	2.369	0.409	0.512	0.000	1.831	7.0	70.96	95.03	78.35	97.53

Table 3. Feed Variation Policies for the PowerFeed Operations Considered in the Analysis of the Effect of Switching Time on Separation Performance (see Figure 6)

	F_1	F_2	F_3
SMB	0.307	0.307	0.307
PF1	0.921	0.000	0.000
PF2	0.800	0.121	0.000
PF3	0.409	0.512	0.000
PF4	0.000	0.921	0.000
PF5	0.100	0.800	0.021
PF6	0.000	0.409	0.512
PF7	0.050	0.050	0.821
PF8	0.000	0.000	0.921

For each PowerFeed variation policy, four switching time values have been considered, namely, the same ones considered for the SMB operation (see, for example, Table 1 and Figure 3). All simulations have been carried with the same values of Q_1, Q_2, Q_4, and an average feed flow rate as those considered in Figure 5. The calculated purity performances are reported in the usual (P_R, P_E) diagram in Figure 6. The reported lines connect operating points corresponding to the same feed variation policy and different t^* values, while the zones with dashed boundaries group together operations sharing the same t^* value. Note that the operating points corresponding to PF1 to PF8 in the zone where $t^* = 6.5$ minutes constitute a subset of those defining the Pareto set in Figure 5a. For a comparison, in the same figure the results corresponding to the SMB simulations in Figure 3 are also shown.

With reference to Figure 6, a few remarks are worthwhile. First, for the SMB, and also in the PowerFeed case, whatever the feed variation policy, increasing t^* leads to a better extract and worse raffinate purity. Second, for a given raffinate purity between 80% and 95%, the SMB extract purity can be increased by choosing a PowerFeed policy among PF1, PF2, PF3, PF4 and PF5, and by slightly decreasing t^*. Third, for a given extract purity between 92% and 94%, the SMB raffinate purity can be increased by choosing a PowerFeed policy within the same set as above, and again by reducing t^*.

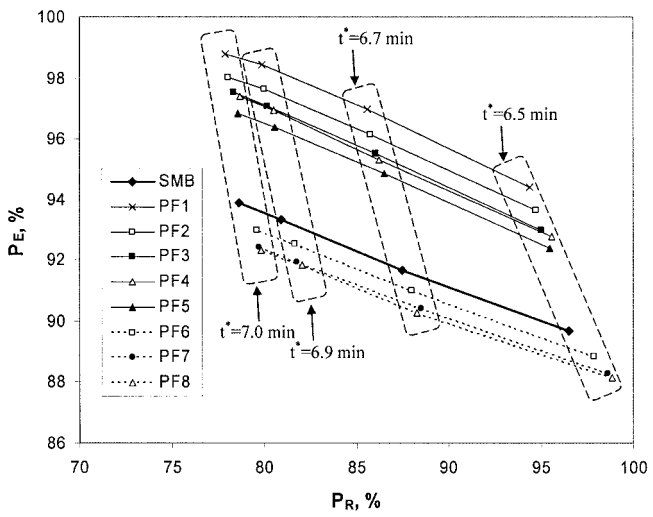

Figure 6. Calculated purity performance of the PowerFeed processes using different *F* variation policies (PF1 to PF8 in Table 3) and of the SMB process, for various values of the switching time.

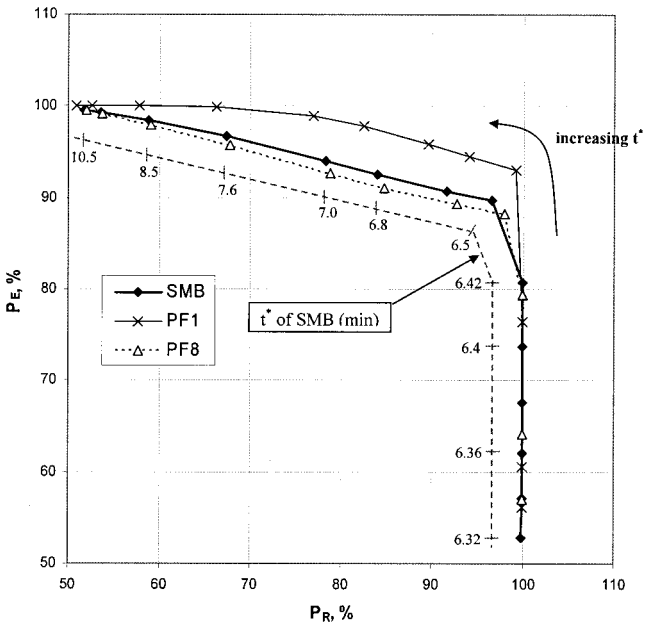

Figure 7. Comparison of the purity performance of the PowerFeed processes with *F* variation policies PF1 and PF8 and of the SMB process for various values of the switching time *t.**

The points along the curves correspond to different t^* values as indicated on the dashed curve for the SMB operation.

The results illustrated in Figure 6 are consistent with those in Figure 5b, in demonstrating that the PowerFeed operation PF1 allows to achieve the best performance in terms of extract purity, whereas the PowerFeed operation PF8 is optimal in terms of raffinate purity. Therefore, these two PowerFeed variation policies are further analyzed and compared to SMB in Figure 7, whereas under the same flow rate conditions as in Figure 6, the purity performances of these three operating modes are investigated over the entire range of feasible t^* values. Such a range is defined with reference to Eq. 1 by a lower bound, below which $\bar{m}_1$ is so small that regeneration in section 1 is no more effective, and the raffinate is polluted by the more retained enantiomer A, and also, an upper bound which is given by the maximum $\bar{m}_4$ value that guarantees a complete regeneration of the fluid stream leaving section 4. In practice, for the system under consideration, the feasible t^* values range from about 6.3 minutes to about 10.5 minutes. The various points on the curves shown in Figure 7 correspond to different t^* values, which increase as P_R decreases, as it is shown for the case of the SMB operation on the dashed curve. It is seen that the PowerFeed policy PF1 always allows to achieve better performances than SMB and PowerFeed PF8. Only for very high P_E or P_R values, the performance of the three processes tends to be very similar. Therefore, as observed in the case of the Varicol operation (Zhang et al., 2002), when high purity of only one product is required, one might not be able to improve the separation performance of SMB by adopting a PowerFeed operation.

In order to verify the theoretical analysis above, PowerFeed experiments with the feed variation policy PF3 in Table 3 were

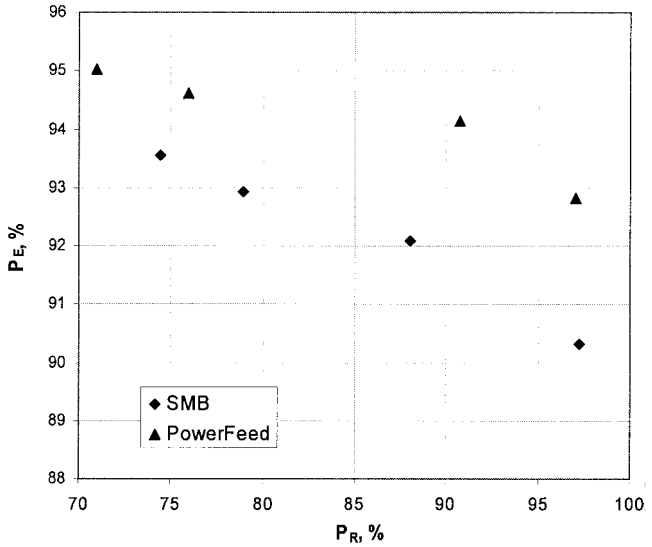

Figure 8. Experimental comparison of the purity performance of PowerFeed (runs P4 to P7 in Table 2) and SMB (runs S1 to S4 in Table 1) processes.

carried out at the same three switching time values used for the SMB operation, that is, $t^* = 6.7$, 6.9 and 7.0 minutes, while Q_1, Q_2, Q_4, and the average Q_3 were kept constant. The corresponding operating conditions and performances are reported in Table 2 (runs P4, P5, P6 and P7). The performances of these PowerFeed runs are compared with that of the corresponding SMB runs S1 to S4 (see Table 1) in Figure 8. The experimental results confirm the theoretical findings, that is, the curve in the (P_R, P_E) plane corresponding to the PF3 PowerFeed operation lies above the corresponding curve for the SMB operation. This implies that the PowerFeed can outperform the SMB with the same desorbent consumption and productivity, provided that the proper switching time value is selected. It is worth noting that at $t^* = 6.7$ minutes (run P5), both the experimental purity values obtained in the PowerFeed run are better than the corresponding ones in the SMB operation (run S2).

Conclusions

In this work we investigate the behavior of the PowerFeed process, which is an extension of the SMB technique where the fluid flow rates are varied in a predefined manner during each time period between two successive switches of the inlet and outlet ports of the unit. Previous theoretical work (Zhang et al., 2003b) had demonstrated that the PowerFeed can achieve a better performance in terms of purity and productivity than SMB, but had not answered the fundamental question about its practical feasibility.

In this article, we investigate the PowerFeed operation experimentally, and compare the measured performances with appropriate chromatographic models. As expected from previous results on the SMB operation, the simulation models are in good agreement with the experiments, which implies that whenever simulations indicate that the PowerFeed outperforms SMB, such performance improvement can also be achieved in practice. This has been shown here in the case of the separation of the enantiomers of α-ionone on a cyclodextrin based stationary phase. A set of SMB experimental runs has been used to estimate the model parameters, namely the adsorption isotherms, and the column efficiency. Such approach for the determination of the adsorption isotherm is unconventional, and certainly leads to a lower accuracy than the traditional methods, based on column pulse or breakthrough experiments. However, we believe that the agreement between the experiments and simulations is satisfactory enough to justify the use of such an approach in the case under examination. The estimated model parameters have been used in an appropriate model to simulate the PowerFeed process and to design its operation conditions, that is, the feed flow rate variation policies. Experimental PowerFeed runs have been carried out to confirm the results of the theoretical analysis, namely that the PowerFeed operation can improve the performance of the classical SMB operation with respect to the purities of both extract and raffinate.

The agreement between the simulation results and experimental data in the case of PowerFeed runs is satisfactory, that is, at least as good as in the case of the SMB experiments used to estimate the model parameters. Moreover, the experimental runs demonstrate that the PowerFeed operation is not affected by difficulties related to the periodic variation of the flow rates of the pumps in the unit. This is an important practical result, since such variations and their potential effects on process robustness have been considered as a potential drawback of PowerFeed compared to SMB and other operation modes, where the pump set points remain constant during the entire operation (with the exception of the recycle pump in some implementations of the SMB technology). As a conclusion, PowerFeed operation can be considered as one of the possible implementations of multicolumn continuous chromatography, which appears particularly attractive for chiral and bio-separations.

Notation

c_i = fluid phase concentration of component i, g/L
c_T^F = total feed concentration, g/L
D = eluent flow rate, mL/min
E = flow rate of extract stream, mL/min
F = feed flow rate, mL/min
$\bar{F}$ = average feed flow rate of PowerFeed, mL/min
H_i = henry constant of component i
J = objective function
K_i = adsorption equilibrium constant of component i
$\bar{m}_j$ = generalized flow rate ratio parameter in section j, defined by Eq. 1
N = number of theoretical stages
P_E = purity of extract stream, %
P_R = purity of raffinate stream, %
q_i = stationary phase concentration of component i, g/L
Q_j = fluid flow rate in section j, mL/min
R = flow rate of raffinate stream, mL/min
t^* = switching time, min
V = column volume, mL
V_j^D = extracolumn dead volume in section j, mL

Greek letters

ε^* = total porosity

Subscripts and superscripts

A = strong component of the feed
B = weak component of the feed

i = component i
j = section j
k = subinterval k

Literature Cited

Abel, S., M. Mazzotti, and M. Morbidelli, "Solvent Gradient Operation of Simulated Moving Beds I. Linear Isotherm," *J. Chromatogr. A.,* **944,** 225 (2002).

Antos, D., and A. Seidel-Morgenstern, "Application of Gradients in the Simulated Moving Bed Process," *Chem. Eng. Sci.,* **56,** 6667 (2001).

Bhaskar, V., S. K. Gupta, and A. K. Ray, "Applications of Multi-Objective Optimization in Chemical Engineering," *Rev. Chem. Eng.,* **16,** 1 (2000).

Denet, F., W. Hauck, R. M. Nicoud, Q. Di Giovanni, M. Mazzotti, J. N. Jaubert, and M. Morbidelli, "Enantioseparation Through Supercritical Fluid Simulated Moving Bed (SF-SMB) Chromatography," *Ind. Eng. Chem. Res.,* **40,** 4603 (2001).

Di Giovanni, O., M. Mazzotti, M. Morbidelli, F. Denet, W. Hauck, and R. M. Nicoud, "Supercritical Fluid Simulated Moving Bed Chromatography II. Langmuir Isotherm," *J. Chromatogr. A.,* **919,** 1 (2001).

Jensen, T. B., T. G. P. Reijns, H. A. H. Billiet, and L. A. M. van der Wielen, "Novel Simulated Moving-Bed Method for Reduced Solvent Consumption," *J. Chromatogr. A.,* **873,** 149 (2000).

Juza, M., M. Mazzotti, and M. Morbidelli, "Simulated Moving-Bed Chromatography and its Application to Chirotechnology," *Trends in Biotechnology,* **18,** 108 (2000).

Kearney, M. M., and K. L. Hieb, "Time Variable Simulated Moving Bed Process," U.S. Patent No. 5 102 553, (1992).

Kloppenburg, E., and E. D. Gilles, "A New Concept for Operating Simulated Moving-bed Processes," *Chem. Eng. Technol.,* **22,** 813 (1999).

Ludemann-Hombourger, O., R. M. Nicoud, and M. Bailly, "The Varicol Process: A New Multicolumn Continuous Chromatographic Process," *Sep. Sci. Technol.,* **35,** 1829 (2000).

Ludemann-Hombourger, O., G. Pigorini, R. M. Nicoud, D. S. Ross, and G. Terfloth, "Application of the "Varicol" Process to the Separation of the Isomers of the SB-553261 Racemate," *J. Chromatogr. A.,* **947,** 59 (2002).

Mazzotti, M., G. Storti, and M. Morbidelli, "Optimal Operation of Simulated Moving Bed Units for Nonlinear Chromatographic Separations," *J. Chromatogr. A.,* **769,** 3 (1997a).

Mazzotti, M., G. Storti, and M. Morbidelli, "Supercritical Fluid Simulated Moving Bed Chromatography," *J. Chromatogr. A.,* **786,** 309 (1997b).

Migliorini, C., M. Mazzotti, and M. Morbidelli, "Simulated Moving-Bed Units with Extra-Column Dead Volume," *AIChE J.,* **45,** 1411 (1999).

Migliorini, C., M. Wendlinger, M. Mazzotti, and M. Morbidelli, "Temperature Gradient Operation of a Simulated Moving Bed Unit," *Ind. Eng. Chem. Res.,* **40,** 2606 (2001).

Nicoud, R. M., G. Hotier, and M. Perrut, "Complex Chromatographic Fractionation Device," French Patent No. FR2690630 (1993).

Pedeferri, M., G. Zenoni, M. Mazzotti, and M. Morbidelli, "Experimental Analysis of a Chiral Separation Through Simulated Moving Bed Chromatography," *Chem. Eng. Sci.,* **54,** 3735 (1999).

Quattrini, F., G. Biressi, M. Juza, M. Mazzotti, C. Fuganti, and M. Morbidelli, "Enantiomer Separation of α-ionone Using Gas Chromatography with Cyclodextrin Derivatives as Chiral Stationary Phases," *J. Chromatogr. A.,* **865,** 201 (1999).

Ruthven, D. M., and C. B. Ching, "Countercurrent and Simulated Countercurrent Adsorption Separation Processes," *Chem. Eng. Sci.,* **44,** 1011 (1989).

Schramn, H., M. Kaspereit, A. Kienle, and A. Seidel-Morgenstern, "Improving Simulated Moving Bed Processes by Cyclic Modulation of the Feed Concentration," *Chem. Eng. Technol.,* **25,** 1151 (2002).

Schramn, H., M. Kaspereit, A. Kienle, and A. Seidel-Morgenstern, "Simulated Moving Bed Process with Cyclic Modulation of the Feed Concentration," *J. Chromatogr. A.,* 1006, 77 (2003).

Storti, G., M. Mazzotti, M. Morbidelli, and S. Carra, "Robust Design of Binary Countercurrent Adsorption Separation Processes," *AIChE J.,* **39,** 471 (1993).

Zenoni, G., F. Quattrini, M. Mazzotti, C. Fuganti, and M. Morbidelli, "Scale-Up of Analytical Chromatography to the Simulated Moving Bed Separation of the Enantiomers of the Flavour Norterpenoids α-Ionone and α-Damascone," *Flavour Frag. J.,* **17,** 195 (2002).

Zang, Y., and P. C. Wankat, "SMB Operation Strategy-Partial Feed," *Ind. Eng. Chem. Res.,* **41,** 2504 (2002a).

Zang, Y., and P. C. Wankat, "Three-Zone Simulated Moving Bed with Partial Feed and Selective Withdrawal," *Ind. Eng. Chem. Res.,* **41,** 5283 (2002b).

Zhang, Z., K. Hidajat, A. K. Ray, and M. Morbidelli, "Multiobjective Optimization of SMB and Varicol Process for Chiral Separation," *AIChE J.,* **48,** 2800 (2002).

Zhang, Z., M. Mazzotti, and M. Morbidelli, "Multiobjective Optimization of Simulated Moving Bed and Varicol Processes Using a Genetic Algorithm," *J. Chromatogr. A.,* **989,** 95 (2003a).

Zhang, Z., M. Mazzotti, and M. Morbidelli, "PowerFeed Operation of SMB Units: Changing the Fluid Flow Rates During the Switching Interval," *J. Chromatogr. A.,* 1006, 87 (2003b).

Manuscript received May 14, 2003, and revision received June 30, 2003.